Environment and Natural Resources Journal

Volume 22
Issue 2
2024

# Monitoring Land Surface Temperature Relationship to Land Use and Land Cover in Hai Duong Province, Vietnam

**Bui B. Thien[1*], Asya E. Ovsepyan[1], and Vu T. Phuong[2,3]**

[1]*Institute of Earth Sciences, Southern Federal University, Rostov-on-Don, 344090, Russian Federation*
[2]*Innovation Startup Support Center, Hong Duc University, Thanh Hoa, 40130, Vietnam*
[3]*Faculty of Social Sciences, Hong Duc University, Thanh Hoa, 40130, Vietnam*

**ARTICLE INFO**

Received: 21 Jul 2023
Received in revised: 21 Jan 2024
Accepted: 23 Jan 2024
Published online: 13 Feb 2024
DOI: 10.32526/ennrj/22/20230194

**Keywords:**
Land surface temperature/ Land use and land cover/ Vegetation cover/ Normalised Difference Vegetation Index/ Hai Duong Province

*** Corresponding author:**
E-mail:
buibaothienha@gmail.com

**ABSTRACT**

This study utilised remote sensing data and ArcGIS 10.8 software to evaluate changes in land use and land cover (LULC) and their effects on land surface temperature (LST) in Hai Duong Province, Vietnam, from 1992 to 2022. Landsat satellite data were pre-processed and classified using supervised methods for the years 1992, 2010, and 2022. In 1992, vegetation cover accounted for 57.89% of land cover, increasing to 84.49% in 2010, but then decreasing again to 66.67% in 2022. In contrast, the built-up area consistently increased, from 2.88% in 1992 to 29.35% in 2022, as most of the barren land present in 1992 became built-up area in 2022. The LST values were calculated from the thermal bands for the years 1992, 2010, and 2022 and ranged from 16.09°C to 34.27°C, 17.04°C to 36.74°C, and 11.03°C to 28.44°C, respectively. In addition, the Normalized Difference Vegetation Index (NDVI) values were calculated using the near-infrared band and the red band, with values ranging from -0.40 to 0.70 over the study period. A linear regression analysis indicated a shift in the correlation between NDVI and LST from positive to negative. This study highlights the significant transformation that occurred in Hai Duong Province due to rapid population density increases, urban growth and infrastructure development, leading to a decline in greenery. These LULC changes can cause severe environmental damage. These research findings will assist policymakers in formulating management strategies and sustainable land-use plans to minimize potential harm and promote sustainable development in the area.

## 1. INTRODUCTION

Climate change has a considerable influence on agriculture, both direct and indirect, making it a significant environmental issue worldwide. Its effects include changes in precipitation patterns, extreme temperature stress and alterations in land surface temperature (LST), which reduce crop health and productivity (Laux et al., 2017; Zia et al., 2017; Praveen and Sharma, 2019; Hammad et al., 2019; Zamin et al., 2019; Celik, 2020; Skendžić et al., 2021). These changes have driven to rural-to-urban migration, significantly affecting land use and land cover (LULC) patterns (Silva et al., 2018; Ritse et al., 2020). Understanding LST patterns is crucial for climate change research and protecting the environment (Donelson et al., 2018; Monroe et al., 2019). Multiple factors, including soil composition, changes in vegetation cover and the presence of permeable and impermeable surfaces, can affect LST patterns. Furthermore, green cover and vegetation play critical roles in mitigating LST in urban areas, making them more resilient to the effects of climate change (Ahmed et al., 2009; Winsemius et al., 2018; Mubeen et al., 2021; Hussain and Karuppannan, 2023).

LULC changes exert a significant influence on the provision of ecosystem services and affect ecosystem functions at the local, regional and global levels (Das and Das, 2019; Li et al., 2021; Phuong and

**Citation:** Thien BB, Ovsepyan AE, Phuong VT. Monitoring land surface temperature relationship to land use and land cover in Hai Duong Province, Vietnam. Environ. Nat. Resour. J. 2024;22(2):145-157. (https://doi.org/10.32526/ennrj/22/20230194)

Thien, 2023a). These changes also affect human variables, such as environmental and political plans (Roberts et al., 2018). Studying LULC changes provides valuable information to understand past practices, current models, and future directions. Change detection techniques, classified by whether they use pixel-, feature- or object-level image processing, are used to categorise LULC changes and different techniques can be used to detect changes (Tang and Di, 2019; Xu et al., 2019; Sahin et al., 2022; Thien et al., 2023a). Earlier research has established that LULC changes can have considerable environmental effects, particularly on the urban climate (Yao et al., 2020; Sahin et al., 2022).

Remote sensing (RS) and geographic information systems (GIS) have proven very effective in analysing and evaluating LULC and LST changes (Owolabi et al., 2020; Hu et al., 2023; Hussain and Karuppannan, 2023; Zeren Cetin et al., 2023). Satellite-based RS provides general LULC data at specific times and locations, and RS and GIS together can be used to map and identify LULC and LST changes. Recently, studies have relied heavily on remote spatial information from satellites to map individual plant species and describe changes in plant types. The Normalised Difference Vegetation Index (NDVI) is essential for monitoring vegetation cover and its response to climate change (Estrella et al., 2021; Fayech and Tarhouni, 2021; Phuong and Thien, 2023b). NDVI values reflect plants' biological activities (Guha, 2021; Bohanon and Crane, 2022). Daily changes in LST can be described through NDVI values, indicating the state of the vegetation cover (Fatemi and Narangifard, 2019; Mukherjee and Singh, 2020; Nse et al., 2020; Hussain and Karuppannan, 2023). NDVI values also help with the study of plants' global and regional ecological cycles. The vegetation response to environmental changes, plant life cycles and vegetation health can all be observed by NDVI (Workie and Debella, 2018; Rizvi et al., 2021; Sajan et al., 2023).

In Vietnam, studies of LST have primarily been conducted in large urban areas, such as Hanoi, Ho Chi Minh City, and Da Nang (Son et al., 2017; Thanh Hoan et al., 2018; Nguyen et al., 2019; Veettil et al., 2023; Veettil and Van, 2023). However, no such work has been performed in the neighbouring areas, such as Hai Duong Province, which are also starting to encounter problems as the expansion of impermeable surface areas causes surface temperatures to rise. Monitoring such issues can help policymakers take early steps to adopt appropriate policies to correct and mitigate the resulting problems. This study's main aim is to investigate the impact of LULC changes on LST in Hai Duong Province from 1992 to 2022 by utilising RS techniques, particularly NDVI. The investigation will also assess the relationship between LULC changes and the effects of climate change in the area. The results will provide policymakers and land managers with essential information to make informed decisions regarding LULC changes in the province. The specific objectives of this study are to (i) assess LULC changes; (ii) calculate LST; (iii) examine changes in vegetation cover using NDVI; and (iv) analyse the relationship between NDVI and LST in Hai Duong Province in 1992, 2010, and 2022.

## 2. METHODOLOGY

### 2.1 Study area

This research focuses on Hai Duong Province located in the Red River Delta region of Vietnam. The province spans approximately 1,668.24 km$^2$, ranging between longitude 106°09′47″ E to 107°04′37″ E and latitude 20°40′38″ N to 21°42′38″ N (General Statistics Office, 2022). It consists of two cities, one town, and nine districts, with Hai Duong City serving as its economic, political, and cultural center. The province is known for its agricultural activities, particularly rice cultivation, due to its relatively flat topography. Additionally, it hosts several industrial zones, such as the Nam Sach and Dai An Industrial Zones, which contribute significantly to its economic growth. The climate of the province is of the tropical monsoon type, featuring warm and humid summers and cool and dry winters. The yearly temperature in the area usually varies between 24 and 26°C, while the average annual precipitation amounts to 1,500-1,800 mm. Natural disasters such as floods, typhoons, and landslides, however, occasionally affect the province's agricultural sector, infrastructure, and people. The study area map was shown in Figure 1.

### 2.2 Landsat data

Satellite images from Landsat 5-TM (1992 and 2010) and Landsat 8-OLI/TIRS (2022) were downloaded freely from the United States Geological Survey (USGS) website (https://earthexplorer.usgs.gov/) (Table 1) to study LULC changes in the study area. A total of six images were downloaded, covering two frames with path/rows of 126/045 and 126/046, and were collected in winter to minimize the impact of cloud cover on the detection of LULC changes. The

LULC model was classified into four groups: vegetation, build-up, barren land, and water bodies, based on field survey information and high-resolution Google Earth Pro images. The accuracy of the LULC classification map was evaluated using 300 points for each year, with samples collected from Google Earth Pro for 1992 and 2010, and field surveys conducted for 2022.

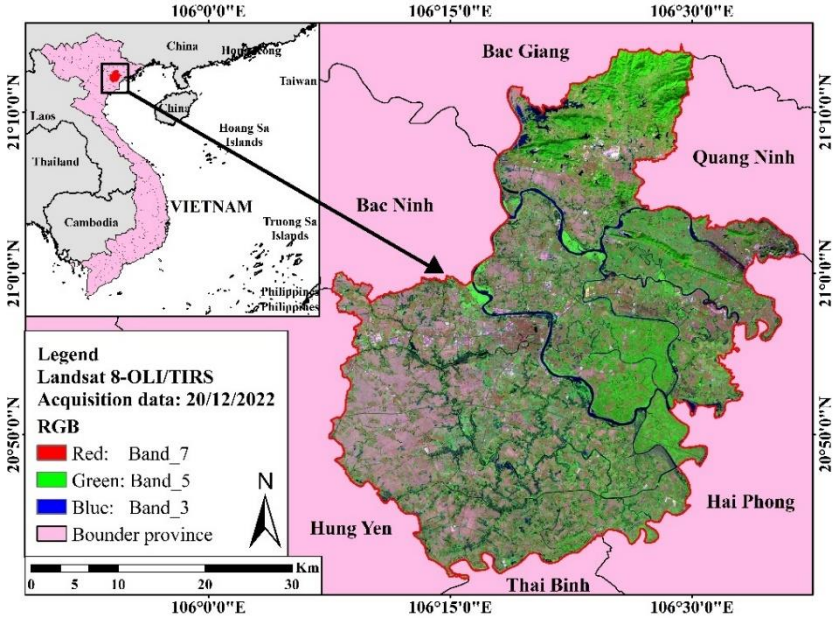


**Figure 1.** Study area map of Hai Duong Province, Vietnam

**Table 1.** Detailed data summary of satellite imagery used in the study

| Landsat scene ID | Acquisition data | Satellite | Image quality | Cloud cover land (%) | Path/row |
|---|---|---|---|---|---|
| LT51260451992336BJC00 | 01/12/1992 | Landsat 5-TM | 9 | 0.00 | 126/045 |
| LT51260461992336BJC00 | | | 7 | 0.00 | 126/046 |
| LT51260452010305BKT00 | 01/11/2010 | Landsat 5-TM | 7 | 0.00 | 126/045 |
| LT51260462010305BKT00 | | | 7 | 0.00 | 126/046 |
| LC81260452022354LGN00 | 20/12/2022 | Landsat 8-OLI/TIRS | 9 | 9.96 | 126/045 |
| LC81260462022354LGN00 | | | 9 | 4.62 | 126/046 |

### 2.3 Image processing and classification

In the preparation of Landsat satellite imagery for this study, co-registering to the UTM zone 48N projection using the WGS-84 datum was essential, accomplished through the utilisation of ArcGIS 10.8 software (Esri, USA) (Thien et al., 2023b). The spectral bands from Landsat 5-TM (bands 1-5 and band 7) and Landsat 8-OLI/TIRS (bands 1-7) were stacked to produce a multiband image using discrete bands (Hussain and Karuppannan, 2023). Mosaicking was then used to combine overlapping images, and the extract by mask tool was used to subset the image based on the study area (Chamling and Bera, 2020; Hussain et al., 2020; Thien et al., 2023b). Once pre-processing was complete, based on local knowledge supervised classification was performed on the satellite image datasets from 1992, 2010, and 2022 using a maximum likelihood algorithm. By drawing polygons around typical locations for each individual LULC type, training samples were chosen for each type (Viana et al., 2019). The spectral signatures of each LULC class were then retrieved from pixels surrounding the delineated polygons (Fayaz et al., 2020; Thien and Phuong, 2023). A detailed methodology is presented in Figure 2.

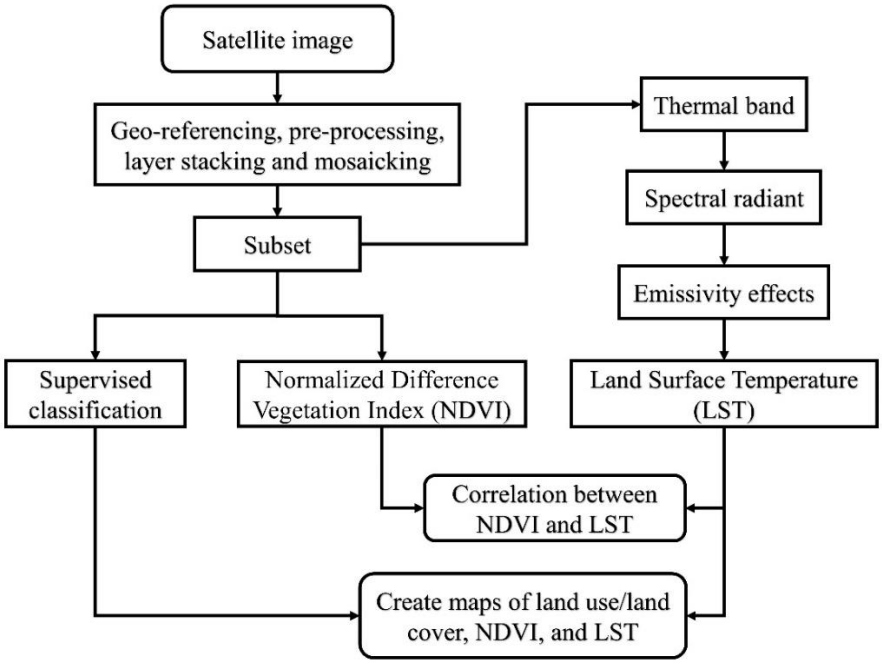


**Figure 2.** Schematic representation of the methodology followed in the study

### 2.4 Accuracy assessment

In this study, a process of accuracy evaluation was carried out to authenticate the generated image classifications and minimize errors in digital imagery (Alganci et al., 2020). Two techniques were utilised to assess accuracy: the error matrix and the kappa coefficient (Feizizadeh et al., 2022; Thien and Phuong, 2023). The error matrix offers the most comprehensive and mutual means of determining the current accuracy outcomes, which can be utilised to derive various statistical measures for accuracy assessment. These include the percentage of the producer's accuracy, the user's accuracy, and overall accuracy, which address errors produced by chance (Hussain et al., 2020). The kappa coefficient, ranging from 0 to 1, expresses the difference between classified results and reference points (Cvitić et al., 2021). Equations (1), (2), (3), and (4) were used as optimal quantitative measures to classify satellite imagery.

$$\text{Producer's accuracy} = \frac{x_{kk}}{x_{+k}} \times 100 \quad (1)$$

$$\text{User's accuracy} = \frac{x_{kk}}{x_{k+}} \times 100 \quad (2)$$

$$\text{Overall accuracy} = \frac{1}{N}\sum_{k=1}^{r} n_i \times 100 \quad (3)$$

$$\text{Kappa coefficient} = \frac{N\sum_{k=1}^{r} x_{kk} - \sum_{k=1}^{r}(x_{k+} . x_{+k})}{N^2 - \sum_{k=1}^{r}(x_{k+} . x_{+k})} \quad (4)$$

Where; N stands for the pixels in total, r for the classes number, and $x_{kk}$ for the sum of the pixels in rows "k" and columns "k", respectively. In the error matrix, the total samples in column "k" are represented by subscription $x_{+k}$, while the total samples in row "k" are represented by $x_{k+}$.

### 2.5 Estimation of NDVI

The NDVI is a widely used criterion for detecting and monitoring vegetation areas (Estrella et al., 2021; Fayech and Tarhouni, 2021). The Landsat images were used to estimate the NDVI, which has values ranging between −1 and +1 (Thien and Phuong, 2023). The NDVI values were calculated using formula (5), which is as follows:

$$\text{NDVI} = \frac{\text{NIR} - \text{RED}}{\text{NIR} + \text{RED}} \quad (5)$$

Where; NIR is the near-infrared band and RED is the red band.

### 2.6 Estimation of LST

The LST is usually measured using the RS technique, which refers to the temperature of the Earth's surface (Zhang et al., 2019). It can be utilised to gain insights into the Earth's energy balance, urban heat island effects, and vegetation stress, among other applications. To compute LST, different researchers

have used defined measurements on Landsat data (Sekertekin and Bonafoni, 2020; Balew and Korme, 2020; Moazzam et al., 2022; Rendana et al., 2023). In this study, LST values were estimated from the thermal bands of Landsat 5-TM and Landsat 8-OLI/TIRS (bands 6 and 10). All steps for the LST calculation are provided below.

Equations (6) and (7) were used to convert digital numbers (DN) to radiance for Landsat 5-TM and Landsat 8-OLI/TIRS, respectively (Rendana et al., 2023).

$$L_\lambda = \left(\frac{L_{max\lambda} - L_{min\lambda}}{QCal_{max} - QCal_{min}}\right) \times (QCal - QCal_{min}) + L_{min\lambda} \quad (6)$$

Where; $L_\lambda$ represents the sensor radiance, $L_{max\lambda}$ is the maximum radiance of band 6, $L_{min\lambda}$ is the minimum radiance of band 6, QCal is the quantized calibrated pixel value in DN, $QCal_{max}$ is the maximum quantized calibrated pixel value in DN, and $QCal_{min}$ is the minimum quantized calibrated pixel value in DN.

$$L_\lambda = M_L \times QCal + A_L \quad (7)$$

Where; $M_L$ is the radiance multiplicative scaling factor, $A_L$ is the radiance additive scaling factor for band10.

Equation (8) was then applied to obtain the Brightness Temperature (BT) in ℃.

$$BT = \left(\frac{K_2}{\ln\left(\frac{K_1}{L_\lambda} + 1\right)}\right) - 273.15 \quad (8)$$

Where; $K_1$ and $K_2$ are the calibration constants of thermal bands (Landsat 5-TM ($K_1$ =607.76 and $K_2$ =1260.56); Landsat 8-OLI/TIRS ($K_1$ =774.8853 and $K_2$=1321.0789)).

Then, equation (9) was utilised to determine the LST.

$$LST = \frac{BT}{1 + \left(\frac{\lambda \times BT}{\rho}\right)} \times \ln(\varepsilon) \quad (9)$$

Where; λ is the central band wavelength of emitted radiance, BT is the Brightness temperature, and ε is the emissivity (evaluated by using equation (10)):

$$\varepsilon = 0.004 \times Pv + 0.986 \quad (10)$$

Where; Pv is the proportion of vegetation evaluated by using equation (11):

$$Pv = \left(\frac{NDVI - NDVI_{min}}{NDVI_{max} - NDVI_{min}}\right)^2 \quad (11)$$

Where; NDVI has been estimated by equation (5).

### 2.7 Regression analysis

Regression analysis was used to measure the correlation between NDVI and LST in Hai Duong Province for the years 1992, 2010, and 2022 (Alam et al., 2022). To perform the regression analysis, 200 random points data were created within the study area boundary using the Create Random Points tool in ArcGIS 10.8. Then, the extract multi values to points tool was used to extract one value for each point from the NDVI and LST pixels (Alam et al., 2022). Finally, these points were exported to Excel 2016 software (Microsoft, USA) to estimate the regression equation between NDVI and LST. The correlation coefficient values generated by the regression analysis ranged from -1 to +1 (Rendana et al., 2023).

## 3. RESULTS AND DISCUSSION

### 3.1 Land use and land cover changes

The study utilised supervised classification techniques to analyse the LULC changes in Hai Duong Province, Vietnam, from 1992 to 2022. The findings indicate that the study area contains diverse land features, such as vegetation, barren land, built-up areas, and bodies of water (Figure 3). In 1992, vegetation accounted for 57.89% (965.71 km$^2$) of the total study area, followed by barren land, which accounted for 35.65% (594.78 km$^2$), water, which accounted for 3.58% (59.76 km$^2$) and, finally, built-up areas, which accounted for at least 2.88% (47.99 km$^2$) (Table 2). By 2010, the vegetation area had increased to 84.49% (1,409.49 km$^2$), while the barren land area had decreased sharply to 4.59% (76.58 km$^2$). The built-up and water areas had also increased to 7.01% (117.02 km$^2$) and 3.91% (65.15 km$^2$), respectively (Table 2). By 2022, the vegetation area had decreased to 66.67% (1,112.23 km$^2$), the barren land area had decreased to only 0.76% (12.73 km$^2$), the built-up area had increased to 29.35% (489.71 km$^2$), and the water area had decreased to 3.21% (53.57 km$^2$) (Table 2). These results show that the built-up area has increased continuously from 1992 to 2022 in the study area.

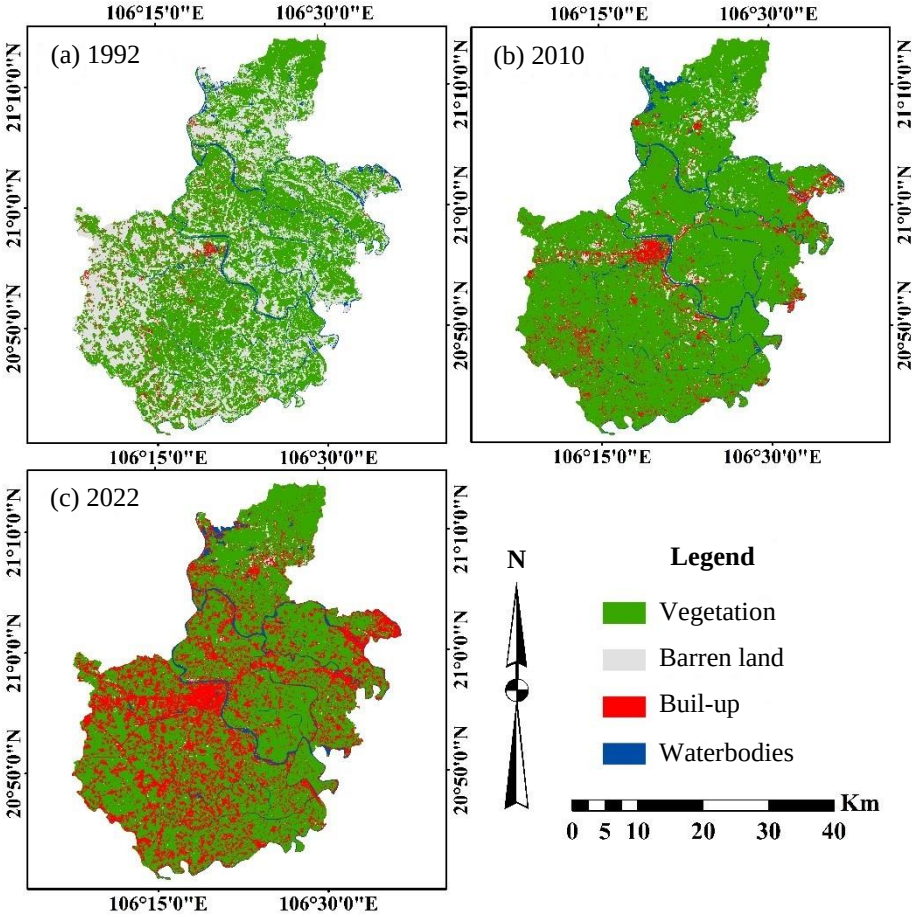


**Figure 3.** Land use/land cover maps of Hai Duong Province in (a) 1992, (b) 2010, and (c) 2022

**Table 2.** Area and percentage of land use/land cover classes distribution in 1992, 2010, and 2022

| LULC classes | 1992 | | 2010 | | 2022 | |
|---|---|---|---|---|---|---|
| | Area ($km^2$) | % | Area ($km^2$) | % | Area ($km^2$) | % |
| Vegetation | 965.71 | 57.89 | 1409.49 | 84.49 | 1112.23 | 66.67 |
| Barren land | 594.78 | 35.65 | 76.58 | 4.59 | 12.73 | 0.76 |
| Built-up | 47.99 | 2.88 | 117.02 | 7.01 | 489.71 | 29.35 |
| Waterbodies | 59.76 | 3.58 | 65.15 | 3.91 | 53.57 | 3.21 |
| Total | 1668.24 | 100.00 | 1668.24 | 100.00 | 1668.24 | 100.00 |

Changes in LULC in Hai Duong Province from 1992 to 2022 are presented in Table 3. From 1992 to 2010, the areas covered by vegetation, built-up areas, and bodies of water increased, while the area of barren land significantly decreased. The vegetation cover experienced the most positive shift, increasing by 443.78 $km^2$ (26.60%), whereas the barren land showed a negative shift, decreasing by 518.20 $km^2$ (31.06%) (Table 3). Meanwhile, the built-up area and bodies of water increased by 69.03 $km^2$ (4.14%) and 5.39 $km^2$ (0.32%), respectively (Table 3). From 2010 to 2022, built-up area showed a strong increasing trend, gaining 372.69 $km^2$ (22.34%), while the other land cover classes, vegetation, barren land, and bodies of water, tended to decrease, losing 297.26 $km^2$ (17.82%), 63.85 $km^2$ (3.83%), and 11.58 $km^2$ (0.69%), respectively (Table 3).

### 3.2 Accuracy assessment

The quality of the LULC maps for the years 1992, 2010, and 2022 was evaluated with an error matrix, which returned overall accuracies of 93.31%, 92.98%, and 96.67%, respectively (Table 4). The producer's accuracy assessment showed that the relative accuracies of land cover classification for 1992 and 2010 were 96.82% and 96.43% for the vegetation category, respectively, and for 2022, the built-up category achieved the highest accuracy

(97.94%) (Table 4). The user accuracy for different land cover classes each year was relatively high. The highest user accuracy occurred in 2010 for the vegetation category (97.59%), while the lowest user accuracy was observed in 1992 for the built-up category (80.77%) (Table 4). The kappa coefficients for 1992, 2010, and 2022 were 0.893, 0.887, and 0.946, respectively (Table 4).

**Table 3.** Land use/land cover changes of Hai Duong Province during 1992-2010, 2010-2022, and 1992-2022

| LULC classes | Changes 1992-2010 | | Changes 2010-2022 | | Changes 1992-2022 | |
|---|---|---|---|---|---|---|
| | Area ($km^2$) | % | Area ($km^2$) | % | Area ($km^2$) | % |
| Vegetation | 443.78 | 26.60 | -297.26 | -17.82 | 146.52 | 8.78 |
| Barren land | -518.20 | -31.06 | -63.85 | -3.83 | -582.05 | -34.89 |
| Built-up | 69.03 | 4.14 | 372.69 | 22.34 | 441.72 | 26.48 |
| Waterbodies | 5.39 | 0.32 | -11.58 | -0.69 | -6.19 | -0.37 |

**Table 4.** Accuracy assessments for classified maps

| LULC classes | 1992 | | 2010 | | 2022 | |
|---|---|---|---|---|---|---|
| | Producer's accuracy (%) | User's accuracy (%) | Producer's accuracy (%) | User's accuracy (%) | Producer's accuracy (%) | User's accuracy (%) |
| Vegetation | 96.82 | 93.83 | 96.43 | 97.59 | 97.39 | 97.39 |
| Barren land | 92.16 | 96.91 | 81.08 | 81.08 | 87.50 | 87.50 |
| Built-up | 87.50 | 80.77 | 94.12 | 96.00 | 97.94 | 96.94 |
| Waterbodies | 83.87 | 89.66 | 88.37 | 82.61 | 92.86 | 95.12 |
| Overall accuracy (%) | 93.31 | | 92.98 | | 96.67 | |
| Kappa coefficient | 0.893 | | 0.887 | | 0.946 | |

### 3.3 NDVI variation in the study area

The NDVI values shifted noticeably over the study period, indicating changes in vegetation and land use. In 1992, the NDVI values in the study area ranged from -0.35 to +0.63, which changed by 2010 to a minimum of -0.40 and a maximum of +0.70 (Figure 4). By 2022, the NDVI values had changed again to a minimum of -0.24 and a maximum of +0.54 in the study area (Figure 4). Higher NDVI values in the study area represent vegetation and forests and signify increased productivity and efficiency, while lower values, associated with bare soil, bodies of water, and built-up areas, indicate reduced productivity.

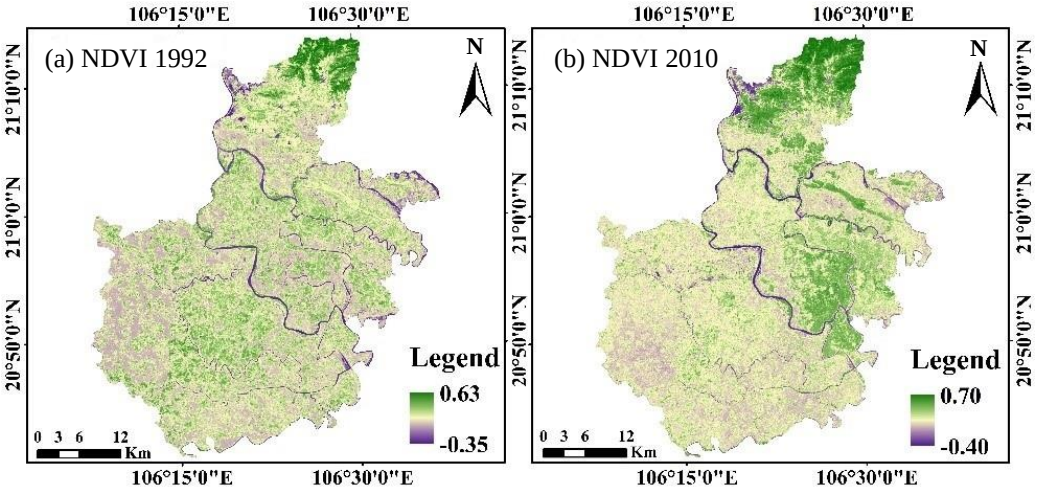


**Figure 4.** The NDVI maps of Hai Duong Province in (a) 1992, (b) 2010, and (c) 2022

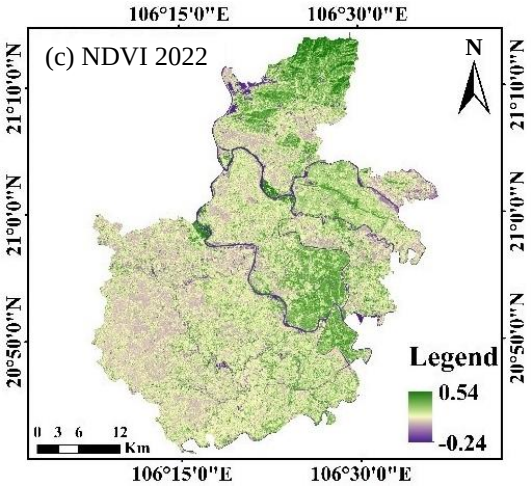


**Figure 4.** The NDVI maps of Hai Duong Province in (a) 1992, (b) 2010, and (c) 2022 (cont.)

### 3.4 LST variation in the study area

Figure 5 presents a visual representation of the spatial distribution and patterns of LST in Hai Duong Province in the three study years (1992, 2010, and 2022) and shows how the LST values and spatial patterns change over time in response to changes in LULC. The estimated LST values ranged from 16.09°C-34.27°C in 1992, 17.04°C-36.74°C in 2010, and 11.03°C-28.44°C in 2022. Notably, LST increased significantly between 1992 and 2010 in most parts of the study area, although some small regions adjacent to water bodies showed stable temperatures. However, by 2022, the overall LST had decreased significantly compared to 1992 and 2010.

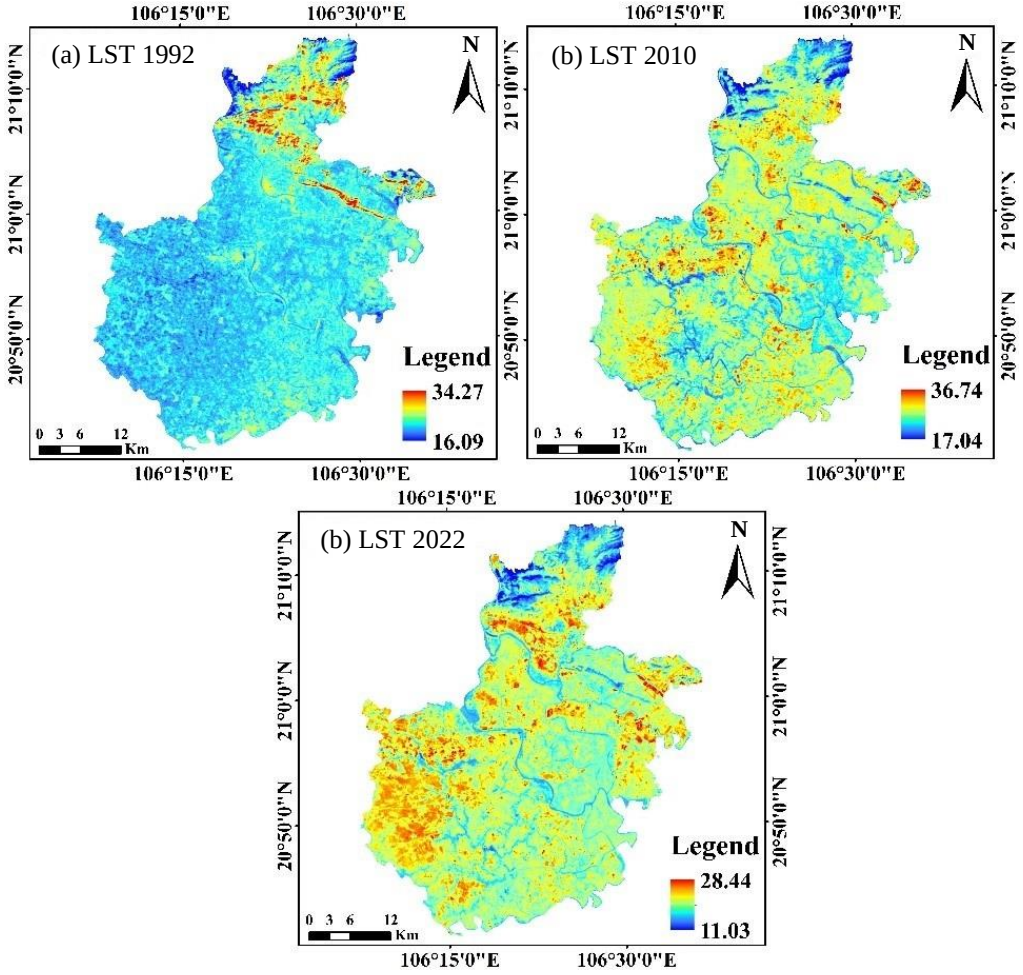


**Figure 5.** The LST maps of Hai Duong Province in (a) 1992, (b) 2010, and (c) 2022

### 3.5 Relationship between NDVI and LST

Figure 6 illustrates the correlation between NDVI and LST during the three study years (1992, 2010, and 2022), with a regression line showing the distinct relationship between these two indices. The correlation coefficients ($R^2$) obtained from linear regression analysis of the data in 1992, 2010, and 2022 were 0.0965, 0.0035, and 0.2277, respectively (Figure 6). The regression line between the NDVI and LST values for the year 1992 indicates a positive correlation; when NDVI values are high, LST values are also high, and vice versa. In 2010, the regression line and correlation coefficient were close to 0, suggesting that NDVI and LST values were less interdependent. However, in 2022, the regression line between these two variables demonstrates a negative correlation. That is, areas with low NDVI values, such as impermeable surfaces and built-up areas, exhibited high LST values, while areas with dense, healthy vegetation have high NDVI values and low LST values.

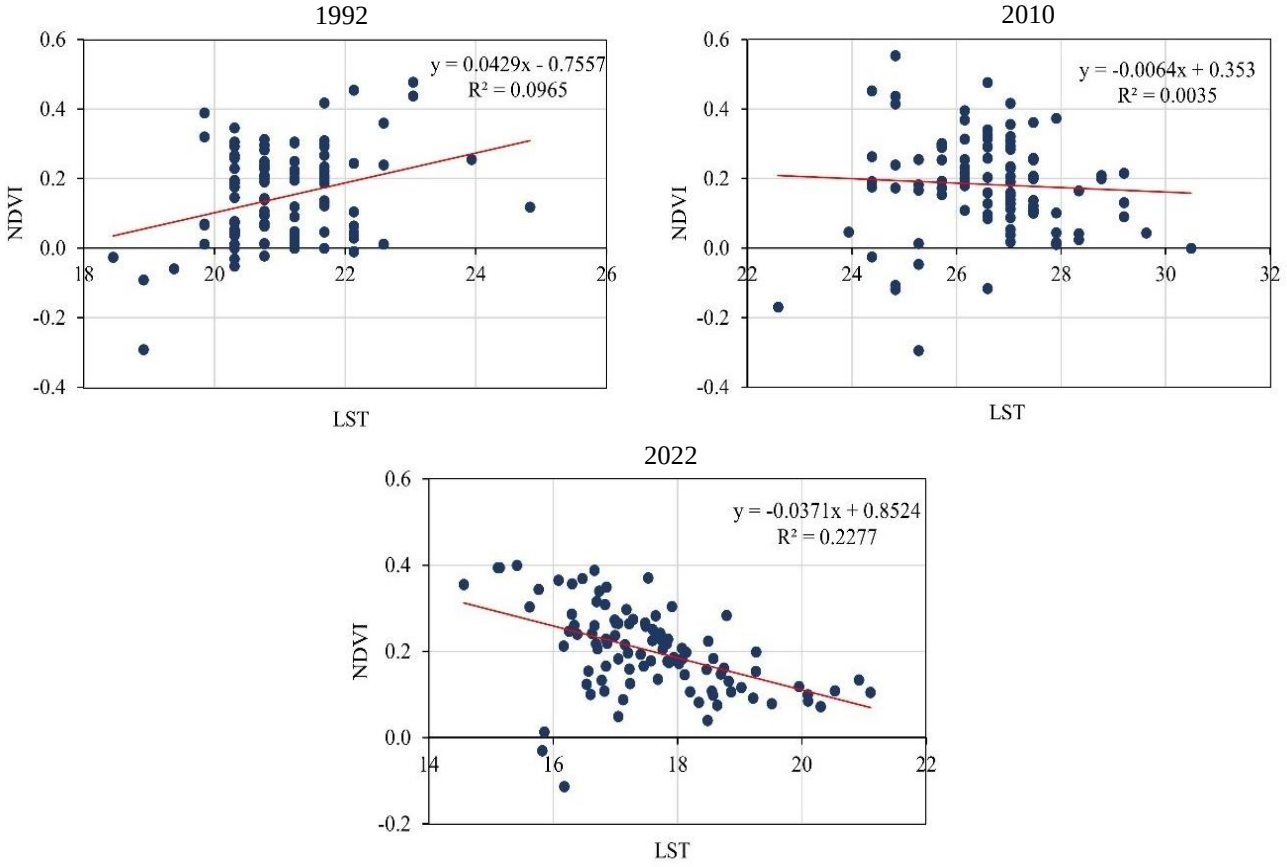


**Figure 6.** Relationship between NDVI and LST for the years 1992, 2010, and 2022 in Hai Duong Province

## 4. DISCUSSION

This study applied modern time- and cost-effective methods to investigate the drivers of LULC and LST changes from 1992 to 2022 in Hai Duong Province, Vietnam. Landsat satellite images (TM and OLI/TIRS) from 1992, 2010, and 2022 were classified using the supervised classification method with four LULC classes, vegetation, barren land, built-up area and bodies of water (Figure 3). The area of each LULC class is also presented in Table 2. Accuracy assessment is important to confirm the correctness of the generated image classifications (Alganci et al., 2020; Hussain et al., 2020; Thien and Phuong, 2023). The classification results were also evaluated for accuracy and returned kappa coefficients above 0.8. These high-accuracy results indicate the reliability of the land cover classification and confirm good consistency between the reference and classification maps. These results confirm that the categorized images meet the necessary accuracy standards and are viable data for subsequent analyses and applications (Cvitić et al., 2021; Thien et al., 2023b).

Spatial analysis of the multi-temporal LULC map of Hai Duong Province shows significant changes over the past 30 years (1992-2022). LULC changes occur continuously and are influenced by many

natural and human factors. These changes have both positive and negative effects. According to socioeconomic reports about Hai Duong Province, the four key economic sectors of the region are agriculture, forestry and fisheries; industry and construction; services; and taxes and subsidies on products. In 2022, the industrial and construction sector accounted for 56.1% of economic activity, while the service sector accounted for 26.5% and the remaining two sectors together only accounted for about 17.0% (Hai Duong Statistical Office, 2022). This suggests that the LULC changes in the study area may reflect the expansion of land used for economic development and urbanization, including the construction of new infrastructure, such as roads, railways, bridges, and industrial zones (Rahaman et al., 2022; Thien et al., 2023a). In addition, climate change may contribute to changes in areas covered by vegetation, barren areas, and bodies of water (Ahmad et al., 2014; Mahmoud and Gan, 2018; Sadiq Khan et al., 2020). The research results highlight the need to implement effective land-use planning and management strategies to minimize the negative effects of these changes on the environment and local communities.

This study was conducted because rapid urbanization has had significant effects on the thermal environment of the study area, which are reflected in the distribution of NDVI and LST values. Using Landsat 5-TM and Landsat 8-OLI/TIRS satellite images, the NDVI index was calculated for the period from 1992 to 2022 by leveraging the spectral characteristics related to vegetation cover, including its ability to absorb visible light, use photosynthetic energy and reflect near-infrared (NIR) radiation (Zeng et al., 2019; Kumar et al., 2022; Thien et al., 2023b). Areas of bare land typically have lower NDVI values than areas with many trees, suggesting the potential effect of increasing vegetation cover as measured by satellite-based assessments of vegetation greenness across the study area. As Ahmad et al. (2014) demonstrated, NDVI is an important component in various vegetation indices due to its stable performance, characterized by non-systematic variation.

These findings highlight the dynamism of LST and its sensitivity to LULC changes. Notably, this study identified a correlation between the expansion of built-up areas and the reduction of vegetation cover, especially in the central and western portions of the study area, leading to increased LSTs in these localities (Balew and Korme, 2020; Alam et al., 2022). These results emphasize the importance of incorporating LULC dynamics into urban planning and management policies to mitigate the adverse effects of urbanization on the local climate and generally improve the quality of life in urban environments (Hussain et al., 2020; Moazzam et al., 2022; Phuong and Thien, 2023a). The deep insights gained from this study can serve as valuable inputs for decision-making processes related to land-use management and planning and contribute to promoting sustainable urban development.

The spatial relationship between NDVI and LST values from 1992-2022 shows that their positive relationship gradually becomes negative. The average LST is low in areas with vegetation cover and flooded areas, indicating a relatively higher rate of water evaporation and favourable conditions for latent exchange between the surface and the atmosphere compared to areas with many impermeable surfaces, such as built-up and barren areas (Thanh Hoan et al., 2018; Rendana et al., 2023; Veettil et al., 2023). Meanwhile, the low NDVI values observed in barren and built-up areas and the high NDVI values seen in areas of mixed vegetation cover and flooded areas reflect a common trend reported in NDVI land cover studies (Alam et al., 2022; Moazzam et al., 2022). The determination coefficient between NDVI and LST values also shows that the positive correlation gradually becomes negative. The density of built-up areas and vegetation cover are important factors determining LST in the study area. The surface density of built-up areas increases LST, while high vegetation cover density significantly reduces LST (Mukherjee and Singh, 2020; Nse et al., 2020).

## 5. CONCLUSION

This study utilised Landsat satellite imagery to assess alterations in LULC and their effects on LST in Hai Duong Province, Vietnam, from 1992 to 2022. The supervised classification method in ArcGIS 10.8 software was used to classify Landsat satellite data, which was evaluated for accuracy and resulted in kappa coefficients of 0.893 for 1992, 0.887 for 2010, and 0.946 for 2022. The classification results showed significant changes in land cover in the study area. Vegetation was the dominant land cover throughout the study period (1992-2022). Meanwhile, the built-up area, which comprised 47.99 $km^2$ (2.88%) in 1992, exhibited a consistent upward trend and eventually reached 489.71 $km^2$ (29.35%) in 2022. The Landsat

data indicated swift changes from barren land in 1992 to vegetation cover in 2010, which then transitioned into built-up area by 2022. Although LST values overall decreased from 34.27°C in 1992 to 28.44°C in 2022, the rising built-up area in Hai Duong Province caused an expansion of high-LST areas in 2022. The regression analysis of NDVI and LST values also showed a shift from a positive to a negative correlation between the two variables. Our study findings suggest that the surge in built-up area and the reduction in bodies of water are among the primary factors contributing to the decline in vegetation cover quality and area, leading to the loss of natural ecosystems and biodiversity. Furthermore, the increasing built-up area may cause further environmental issues. The evaluation of LULC changes can help define the effects of various development activities on LULC classes during the planning process. The use of RS and GIS technologies also enables spatiotemporal analysis, which cannot be achieved through conventional mapping techniques. This study will enhance local and national authorities' ability to develop comprehensive strategies for land management in the study area.

The use of satellite imagery, while beneficial for large-scale analysis, may not capture the fine details of land use and land cover changes that occur at a smaller scale. For future studies, the inclusion of socioeconomic data could provide a more comprehensive understanding of the drivers of the observed LULC changes. Long-term monitoring and prediction models could also be developed to forecast future LULC changes and their potential effects on the local climate and biodiversity. These recommendations, if implemented, could result in more robust and comprehensive insights into land use and land cover changes and their implications for sustainable urban development.

## REFERENCES


Ahmad F, Ghazi S, Ahmad SR, Ahmad I, Khan RMA, Raoof A, et al. Spectral characteristics and mapping of rice fields using multi-temporal landsat and MODIS data: A case of District Narowal. Global Journal of Human-Social Science Research 2014;14(6):Article No. 2.

Ahmed J, Ahmed M, Laghari A, Lohana W, Ali S, Fatmi Z. Public private mix model in enhancing tuberculosis case detection in District Thatta, Sindh, Pakistan. Journal of the Pakistan Medical Association 2009;59(2):Article No. 82.

Alam HE, Arafat MdY, Ahmed KT, Uddin MN. Temporal variation of land surface temperature in response to changes in vegetation index of Bhawal National Park, Bangladesh. In: Pal I, Kolathayar S, editors. Sustainable Cities and Resilience. Singapore: Lecture Notes in Civil Engineering Springer Singapore; 2022. p. 329-37.

Alganci U, Soydas M, Sertel E. Comparative research on deep learning approaches for airplane detection from very high-resolution satellite images. Remote Sensing 2020;12(3): Article No. 458.

Balew A, Korme T. Monitoring land surface temperature in Bahir Dar City and its surrounding using landsat images. The Egyptian Journal of Remote Sensing and Space Science 2020;23(3):371-86.

Bohanon A, Crane K. Structural and biological analysis of faults in basalts in Sheepshead Mountains, Oregon as an earth analogue to mars. Icarus 2022;385:Article No. 115121.

Celik S. The effects of climate change on human behaviors. In: Fahad S, Hasanuzzaman M, Alam M, Ullah H, Saeed M, Khan IA, et al. editors. Environment, Climate, Plant and Vegetation Growth. Cham: Springer International Publishing; 2020; p. 577-89.

Chamling M, Bera B. Spatio-temporal patterns of land use/land cover change in the Bhutan-Bengal Foothill region between 1987 and 2019: Study towards geospatial applications and policy making. Earth Systems and Environment 2020;4(1): 117-30.

Cvitić I, Peraković D, Periša M, Gupta B. Ensemble machine learning approach for classification of IoT devices in smart home. International Journal of Machine Learning and Cybernetics 2021;12(11):3179-202.

Das M, Das A. Dynamics of urbanization and its impact on urban ecosystem services (UESs): A study of a medium size town of West Bengal, Eastern India. Journal of Urban Management 2019;8(3):420-34.

Donelson JM, Salinas S, Munday PL, Shama LN. Transgenerational plasticity and climate change experiments: Where do we go from here? Global Change Biology 2018;24(1):13-34.

Estrella EH, Stoeth A, Krakauer NY, Devineni N. Quantifying vegetation response to environmental changes on the Galapagos Islands, Ecuador using the normalized difference vegetation index (NDVI). Environmental Research Communications 2021;3(6):Article No. 065003.

Fatemi M, Narangifard M. Monitoring LULC changes and its impact on the LST and NDVI in district 1 of Shiraz City. Arabian Journal of Geosciences 2019;12(4):Article No. 127.

Fayaz A, Shafiq MU, Singh H, Ahmed P. Assessment of spatiotemporal changes in land use/land cover of North Kashmir Himalayas from 1992 to 2018. Modeling Earth Systems and Environment 2020;6(2):1189-200.

Fayech D, Tarhouni J. Climate variability and its effect on normalized difference vegetation index (NDVI) using remote sensing in semi-arid area. Modeling Earth Systems and Environment 2021;7(3):1667-82.

Feizizadeh B, Darabi S, Blaschke T, Lakes T. QADI as a new method and alternative to Kappa for accuracy assessment of remote sensing-based image classification. Sensors 2022; 22(12):Article No. 4506.

General Statistics Office. Statistical yearbook of Viet Nam. Statistical publishing house [Internet]. 2022 [cited 2023 Jul 10]. Available from: https://www.gso.gov.vn/wp-content/uploads/2023/06/Sach-Nien-giam-TK-2022-update-21.7_file-nen-Water.pdf.

Guha S. Dynamic seasonal analysis on LST-NDVI relationship and ecological health of Raipur City, India. Ecosystem Health and Sustainability 2021;7(1):Article No. 1927852.

Hai Duong Statistical Office. Report: Socio-economic situation in December and the whole year of 2022, Hai Duong province [Internet]. 2022 [cited 2023 Jul 10]. Available from: https://web01.haiduong.gov.vn/Lists/TinTuc/Attachments/14460/BC%20KTXH%20T12.2022%20tinh%20Hai%20Duong.pdf.

Hammad HM, Ashraf M, Abbas F, Bakhat HF, Qaisrani SA, Mubeen M, et al. Environmental factors affecting the frequency of road traffic accidents: A case study of sub-urban area of Pakistan. Environmental Science and Pollution Research 2019;26(12):11674-85.

Hu Y, Raza A, Syed NR, Acharki S, Ray RL, Hussain S, et al. Land use/land cover change detection and NDVI estimation in Pakistan's Southern Punjab Province. Sustainability 2023; 15(4):Article No. 3572.

Hussain S, Karuppannan S. Land use/land cover changes and their impact on land surface temperature using remote sensing technique in District Khanewal, Punjab Pakistan. Geology, Ecology, and Landscapes 2023;7(1):46-58.

Hussain S, Mubeen M, Ahmad A, Akram W, Hammad HM, Ali M, et al. Using GIS tools to detect the land use/land cover changes during forty years in Lodhran District of Pakistan. Environmental Science and Pollution Research 2020;27 (32):39676-92.

Kumar S, Arya S, Jain K. A SWIR-based vegetation index for change detection in land cover using multi-temporal landsat satellite dataset. International Journal of Information Technology 2022;14(4):2035-48.

Laux P, Nguyen PNB, Cullmann J, Kunstmann H. Impacts of land-use/land-cover change and climate change on the regional climate in the Central Vietnam. In: Nauditt A, Ribbe L. editors. Land Use and Climate Change Interactions in Central Vietnam: Water Resources Development and Management. Singapore: Springer Singapore; 2017. p. 143-51.

Li C, Wu Y, Gao B, Zheng K, Wu Y, Li C. Multi-scenario simulation of ecosystem service value for optimization of land use in the sichuan-yunnan ecological barrier, China. Ecological Indicators 2021;132:Article No. 108328.

Mahmoud SH, Gan TY. Impact of anthropogenic climate change and human activities on environment and ecosystem services in arid regions. Science of the Total Environment 2018; 633:1329-44.

Moazzam MFU, Doh YH, Lee BG. Impact of urbanization on land surface temperature and surface urban heat island using optical remote sensing data: A case study of Jeju Island, Republic of Korea. Building and Environment 2022;222:Article No. 109368.

Monroe MC, Plate RR, Oxarart A, Bowers A, Chaves WA. Identifying effective climate change education strategies: A systematic review of the research. Environmental Education Research 2019;25(6):791-812.

Mubeen M, Bano A, Ali B, Islam ZU, Ahmad A, Hussain S, et al. Effect of plant growth promoting bacteria and drought on spring maize (*Zea Mays* L.). Pakistan Journal of Botany 2021;53(2):731-9.

Mukherjee F, Singh D. Assessing land use-land cover change and its impact on land surface temperature using LANDSAT data: A comparison of two urban areas in India. Earth Systems and Environment 2020;4(2):385-407.

Nguyen TM, Lin TH, Chan HP. The environmental effects of urban development in Hanoi, Vietnam from satellite and meteorological observations from 1999-2016. Sustainability 2019;11(6):Article No. 1768.

Nse OU, Okolie CJ, Nse VO. Dynamics of land cover, land surface temperature and NDVI in Uyo City, Nigeria. Scientific African 2020;10:e00599.

Owolabi ST, Madi K, Kalumba AM, Orimoloye IR. A groundwater potential zone mapping approach for semi-arid environments using remote sensing (RS), geographic information System (GIS), and Analytical Hierarchical Process (AHP) techniques: A case study of buffalo catchment, Eastern Cape, South Africa. Arabian Journal of Geosciences 2020;13(22):Article No. 1184.

Phuong VT, Thien BB. A multi-temporal landsat data analysis for land-use/land-cover change in the Northwest Mountains Region of Vietnam Using Remote Sensing Techniques. Forum Geografic 2023a;22(1):54-66.

Phuong VT, Thien BB. Using landsat satellite images to detect forest cover changes in the Northeast Region of Vietnam. Bulletin of the Transilvania University of Brasov Series II: Forestry Wood Industry Agricultural Food Engineering 2023b;16(1):19-36.

Praveen B, Sharma P. A review of literature on climate change and its impacts on agriculture productivity. Journal of Public Affairs 2019;19(4):e1960.

Rahaman ZA, Kafy AA, Faisal AA, Al Rakib A, Jahir DMA, Fattah MA, et al. Predicting microscale land use/land cover changes using cellular automata algorithm on the Northwest Coast of Peninsular Malaysia. Earth Systems and Environment 2022;6(4):817-35.

Rendana M, Razi Idris WM, Abdul Rahim S, Ghassan Abdo H, Almohamad H, Abdullah Al Dughairi A, et al. Effects of the built-up index and land surface temperature on the mangrove area change along the Southern Sumatra Coast. Forest Science and Technology 2023;19(3):179-89.

Ritse V, Basumatary H, Kulnu AS, Dutta G, Phukan MM, Hazarika N. Monitoring land use land cover changes in the Eastern Himalayan Landscape of Nagaland, Northeast India. Environmental Monitoring and Assessment 2020;192(11): Article No. 711.

Rizvi SH, Fatima H, Alam K, Iqbal MJ. The surface urban heat island intensity and urban expansion: A comparative analysis for the Coastal Areas of Pakistan. Environment, Development and Sustainability 2021;23(4):5520-37.

Roberts C, Geels FW, Lockwood M, Newell P, Schmitz H, Turnheim B, et al. The politics of accelerating low-carbon transitions: Towards a new research agenda. Energy Research and Social Science 2018;44:304-11.

Sadiq Khan M, Ullah S, Sun T, Rehman AU, Chen L. Land-use/land-cover changes and its contribution to urban heat island: A case study of Islamabad, Pakistan. Sustainability 2020;12(9):Article No. 3861.

Sahin G, Cabuk SN, Cetin M. The change detection in coastal settlements using image processing techniques: A case study of Korfez. Environmental Science and Pollution Research 2022;29(10):15172-87.

Sajan B, Kanga S, Singh SK, Mishra VN, Durin B. Spatial variations of LST and NDVI in Muzaffarpur District, Bihar using google earth engine (GEE) during 1990-2020. Journal of Agrometeorology 2023;25(2):262-7.

Sekertekin A, Bonafoni S. Sensitivity analysis and validation of daytime and nighttime land surface temperature retrievals from landsat 8 using different algorithms and emissivity models. Remote Sensing 2020;12(17):Article No. 2776.

Silva JS, da Silva RM, Santos CAG. Spatiotemporal impact of land use/land cover changes on urban heat islands: A case study of Paço Do Lumiar, Brazil. Building and Environment 2018;136:279-92.

Skendžić S, Zovko M, Živković IP, Lešić V, Lemić D. The impact of climate change on agricultural insect pests. Insects 2021;12(5):Article No. 440.

Son NT, Chen CF, Chen CR, Thanh BX, Vuong TH. Assessment of urbanization and urban heat islands in Ho Chi Minh City, Vietnam using landsat data. Sustainable Cities and Society 2017;30:150-61.

Tang J, Di L. Past and future trajectories of farmland loss due to rapid urbanization using landsat imagery and the markov-CA model: A case study of Delhi, India. Remote Sensing 2019;11(2):Article No. 180.

Thanh Hoan N, Liou YA, Nguyen KA, Sharma RC, Tran DP, Liou CL, et al. Assessing the effects of land-use types in surface urban heat islands for developing comfortable living in Hanoi City. Remote Sensing 2018;10(12):Article No. 1965.

Thien BB, Phuong VT. Using landsat satellite imagery for assessment and monitoring of long-term forest cover changes in Dak Nong Province, Vietnam. Geographica Pannonica 2023;27(1):69-82.

Thien BB, Phuong VT, Komolafe AA. Assessment of forest cover and forest loss using satellite images in Thua Thien Hue Province, Vietnam. AUC Geographica 2023a;58(2):172-86.

Thien BB, Yachongtou B, Phuong VT. Long-term monitoring of forest cover change resulting in forest loss in the capital of Luang Prabang Province, Lao PDR. Environmental Monitoring and Assessment 2023b;195(8):Article No. 947.

Veettil BK, Puri V, Van DD, Quang NX. Variations in land surface temperatures in small-scale urban areas in Vietnam during Covid-19 restrictions: Case studies from Da Nang, Hue and Vinh City. Environmental Monitoring and Assessment 2023;195(7):Article No. 822.

Veettil BK, Van DD. Did the Covid-19 restrictions influence land surface temperatures in Southeast Asia? A study from Ho Chi Minh City, Vietnam. Environmental Science and Pollution Research 2023;30(25):66812-21.

Viana CM, Girão I, Rocha J. Long-term satellite image time-series for land use/land cover change detection using refined open source data in a rural region. Remote Sensing 2019;11(9): Article No. 1104.

Winsemius HC, Jongman B, Veldkamp TI, Hallegatte S, Bangalore M, Ward PJ. Disaster risk, climate change, and poverty: Assessing the global exposure of poor people to floods and droughts. Environment and Development Economics 2018;23(3):328-48.

Workie TG, Debella HJ. Climate change and its effects on vegetation phenology across ecoregions of ethiopia. Global Ecology and Conservation 2018;13:e00366.

Xu L, Jing W, Song H, Chen G. High-resolution remote sensing image change detection combined with pixel-level and object-level. IEEE Access 2019;7:78909-18.

Yao N, Huang C, Yang J, Konijnendijk van den Bosch CC, Ma L, Jia Z. Combined effects of impervious surface change and large-scale afforestation on the surface urban heat island intensity of Beijing, China based on remote sensing analysis. Remote Sensing 2020;12(23):Article No. 3906.

Zamin M, Khattak AM, Salim AM, Marcum KB, Shakur M, Shah S, et al. Performance of aeluropus lagopoides (mangrove grass) ecotypes, a potential turfgrass, under high saline conditions. Environmental Science and Pollution Research 2019;26(13):13410-21.

Zeng Y, Badgley G, Dechant B, Ryu Y, Chen M, Berry JA. A practical approach for estimating the escape ratio of near-infrared solar-induced chlorophyll fluorescence. Remote Sensing of Environment 2019;232:Article No. 111209.

Zeren Cetin I, Varol T, Ozel HB. A geographic information systems and remote sensing-based approach to assess urban micro-climate change and its impact on human health in Bartin, Turkey. Environmental Monitoring and Assessment 2023;195(5):Article No. 540.

Zhang X, Zhou J, Göttsche F-M, Zhan W, Liu S, Cao R. A method based on temporal component decomposition for estimating 1-Km all-weather land surface temperature by merging satellite thermal infrared and passive microwave observations. IEEE Transactions on Geoscience and Remote Sensing 2019;57(7):4670-91.

Zia Z, Bakhat HF, Saqib ZA, Shah GM, Fahad S, Ashraf MR, et al. Effect of water management and silicon on germination, growth, phosphorus and arsenic uptake in rice. Ecotoxicology and Environmental Safety 2017;144:11-8.